



# On-line chip speed measurement in the turning process

A. M. G. Boeira<sup>1</sup>, J. T. Gomes<sup>1</sup>, R. Margot<sup>1</sup>, F. Kuster<sup>1</sup>, H. Roelofs<sup>2</sup>, U. Urlau<sup>2</sup>, W. L. Weingaertner<sup>3</sup>

<sup>1</sup> *Institute of Machine Tools and Manufacturing, Department for Mechanical and Process Engineering, Swiss Federal Institute of Technology, 8092 Zürich, SWITZERLAND*

<sup>2</sup> *von Moos Stahl, 6021 Emmenbrücke, SWITZERLAND*

<sup>3</sup> *Laboratory of Precision Mechanics, Department of Mechanical Engineering, Federal University of Santa Catarina, 88040-970 Florianópolis, BRASIL*

The 38<sup>th</sup> CIRP International Seminar on Manufacturing Systems May 16/18 - 2005

# On-line chip speed measurement in the turning process

A. M. G. Boeira<sup>1</sup>, J. T. Gomes<sup>1</sup>, R. Margot<sup>1</sup>, F. Kuster<sup>1</sup>, H. Roelofs<sup>2</sup>, U. Urlau<sup>2</sup>, W. L. Weingaertner<sup>3</sup>

<sup>1</sup> Institute of Machine Tools and Manufacturing, Department for Mechanical and Process Engineering, Swiss Federal Institute of Technology, Zurich, Switzerland

<sup>2</sup> von Moos Stahl, Emmenbrücke, Switzerland

<sup>3</sup> Laboratory of Precision Mechanics, Department of Mechanical Engineering, Federal University of Santa Catarina, Florianópolis, Brasil

## Abstract

On-line measurements of temperature, forces and acoustic emission signals give detailed real time information about the interaction between tool and material. This paper presents a new and fast procedure to gain on-line information about the chip velocity during machining without using mathematical models. The chip velocity is determined using the focus spots of two pyrometers on the chip surface defining a suitable distance. Observing the characteristic temperature profile of the chip moving through these two barriers gives the time delay by cross correlating temperature signals. From the chip velocity and the cutting speed, the chip thickness and the shear plane angle can be deduced.

## Keywords:

Machinability, Chip speed, Free cutting steel, Monitoring

## 1 INTRODUCTION

Machinability is an outstanding steel property. Therefore it is not surprising that many machinability tests currently exist, of which the most commonly used is ISO 3685 [1]. These conventional tests typically consume large amounts of steel and time. Due to this only few tests are typically performed leading to poor statistics and modest insight in the physics of the machining process. In order to get faster information with more statistical relevance new reliable machinability tests based on on-line data acquisition should be developed. Recent research work has been successfully done on acoustic emission techniques achieving information about chip breaking [2,3], friction [3,4] and plastic deformation [3]. Additionally the present work focuses on the on-line measurement of the shear plane angle. In the past the shear plane angle could be obtained by very expensive quick-stop investigations [5,6] or by measuring the chip thickness and using simple geometrical relations. This latter method can be replaced by an on-line measurement if it succeeds in detecting the chip speed at the vicinity of chip formation. This paper presents a new strategy to gain this information on-line in a single point turning test by using two high response pyrometers with subsequent advanced signal analyses. First data sets of three different free cutting steel grades were compared with results based on off-line chip thickness measurements.

## 2 THEORY

The chip is formed by the tool-workpiece interaction. As the edge of the tool penetrates into the workpiece, the material ahead of the tool is sheared. The sheared material or chip partially deforms and moves along the rake face of the tool. The high strain rates modify the chip cross-section [7,8,9,10,11]. The cutting analyses at the tool-workpiece-chip interfaces show the existence of 4 zones according to figure 1 [12]:

1. The primary shearing zone.
2. The secondary shearing zone.
3. The principal and secondary clearance zone.
4. The dead zone.

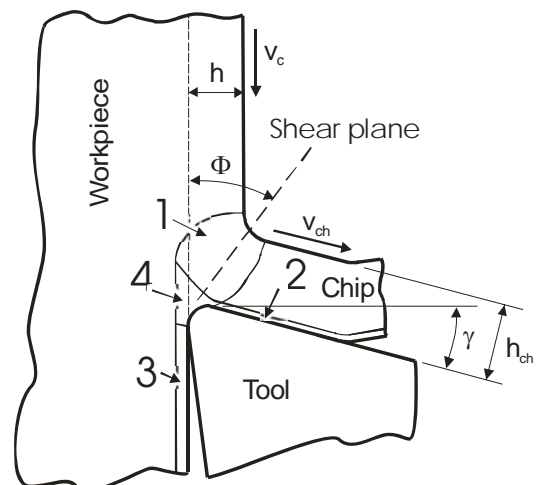


Figure 1: Chip formation main zones.

Where:

$h$  = Undeformed chip thickness.

$h_{ch}$  = Chip thickness.

$v_c$  = Cutting speed.

$v_{ch}$  = Chip speed.

$\gamma$  = Rake angle.

$\Phi$  = Shear angle.

In the primary shearing zone the material is sheared and the chip is formed. This zone is characterized by the shear plane. The angle between this shear plane and the cutting speed direction gives the called shear angle ( $\Phi$ ). In the secondary shearing zone, the chip is pressed and moves along the rake face of the tool with a velocity ( $v_{ch}$ ). In the principal and secondary clearance zone, the tool penetrates in the workpiece and rubs the newly machined surface. The material remains in an elastic state. In the dead zone, the material is divided into two parts. One will

constitute the new outer surface of the workpiece, the second will be chipped [9,12].

The chip formation was analysed by Ernst and Merchant using the thin shear-zone model, assuming that the cutting edge is sharp without a chamfer or radius and that the deformation takes place at the infinitely thin shear plane [9,10,11,12]. The relation between the different forces respectively the velocities in this model is shown in the figure 2.

The shear angle ( $\phi$ ) is defined as the angle between the direction of the cutting speed ( $v_c$ ) and the shear plane [7,8,9,10,11,12].

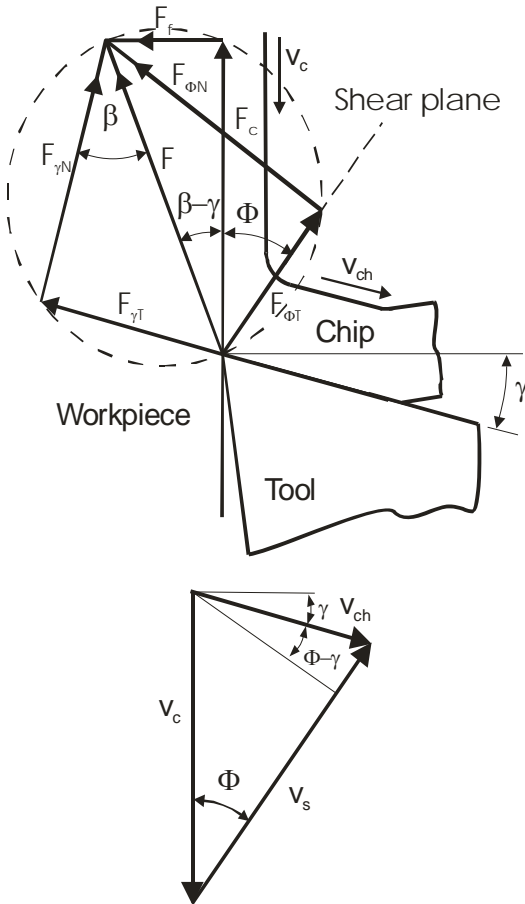


Figure 2: Forces and velocities diagrams.

Where:

- $F$  = Resultant force.
- $F_c$  = Cutting force.
- $F_f$  = Thrust force.
- $F_{\gamma T}$  = Friction force.
- $F_{\gamma N}$  = Normal force.
- $F_{\phi T}$  = Shear force.
- $F_{\phi N}$  = Normal force acting on the shear plane.
- $v_s$  = Shear velocity.
- $\beta$  = Friction angle on tool face.

The shear angle of the cutting process defines the chip thickness (Equation 1). Thinner chips can be achieved by an increase of this angle due an increase of the rake angle of cutting tool or by a decrease of friction coefficient between the tool face and the chip [14].

$$h_{ch} = \frac{\cos(\Phi - \gamma)}{\sin(\Phi)} \cdot h \quad (1)$$

Equation 2 uses the chip compression ( $\lambda_h$ ) as the relation between the real and the undeformed chip thicknesses or between cutting speed and chip speed [3, 13, 14].

$$\lambda_h = \frac{h_{ch}}{h} = \frac{v_c}{v_{ch}} \quad (2)$$

Replacing the thickness in equation 1, the chip speed ( $v_{ch}$ ) and the shear angle ( $\phi$ ) can be defined by equation 3 [14,15].

$$v_{ch} = \frac{\sin(\Phi)}{\cos(\Phi - \gamma)} \cdot v_c \quad (3)$$

### 3 EXPERIMENTAL PROCEDURE

A standard turning machine (Schäublin 42L) was equipped with a new developed optical device (Figure 3) to monitor the temperature of the chips.

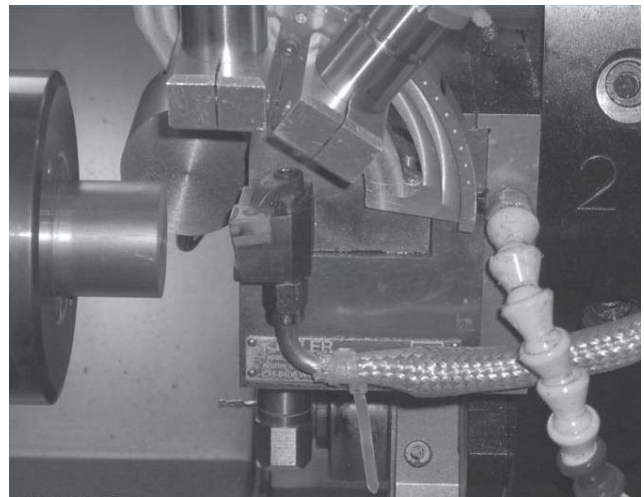


Figure 3: Pyrometer configuration in the turning machine.

#### 3.1 Principle

The temperature distribution in the chip during orthogonal cutting can be measured with infrared photograph [5,10] or as a time signal with a pyrometer. Measuring the temperature on the chip surface, severe fluctuations are expected due to the surface roughness and due to chip breaks. Therefore a pyrometer focusing on a fixed position  $B$  (Figure 4) on the chip surface will register a typical temperature function. A second pyrometer focusing on a position  $C$  in distance ( $ds$ ) of position  $B$  will observe the same temperature profile at a later time. Applying a cross correlation [16,17] to these two measured functions the time delay ( $dt$ ) can be deduced. If the referred distance ( $ds$ ) between  $B$  and  $C$  is known, the chip speed can be calculated with equation 4.

$$v_{ch} = \frac{ds}{dt} \quad (4)$$

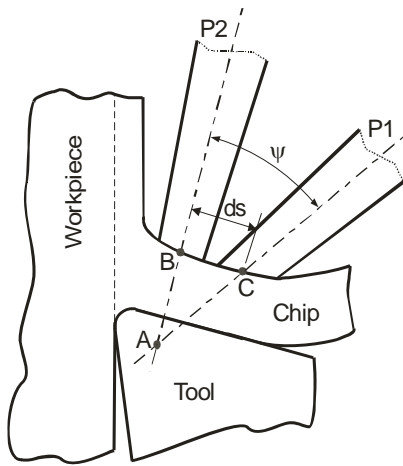


Figure 4: Distance determination with geometrical model.

Where:

P1 = Pyrometer 1.

P2 = Pyrometer 2.

ds = Measurement distance.

### 3.2 Construction

To measure the chip velocity it is needed to guarantee that the focuses of both pyrometers are on a plain region of the chip.

Parallel alignment of both pyrometers could facilitate the determination of the distance of measurement. However, the optics diameters limit the distance ( $ds$ ) to a minimum of 25 mm. This is far too large. The distance ( $ds$ ) should be as small as possible to reduce geometrical errors due to the chip curvature. Therefore the pyrometers were mounted with an angle ( $\psi$ ) between themselves as shown in Figure 5. As a consequence of this arrangement the distance of the two spots on the chip surface becomes dependent on the chip thickness itself. In a first assumption this effect has been neglected (in case of similar steel grades and fixed cutting speed this assumption should be reasonable).

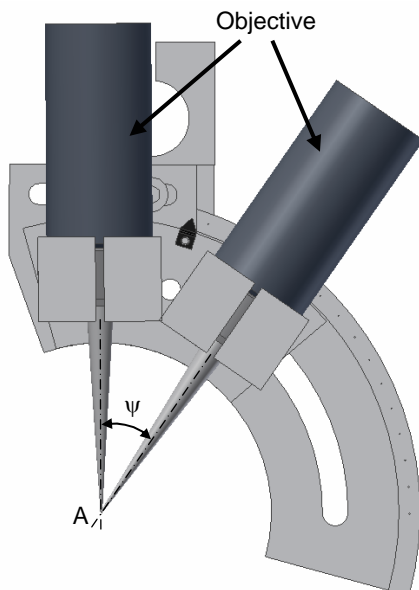


Figure 5: Objectives assembly.

The method applied in the  $ds$  determination consists in multiplying the time delay obtained from the cross correlation of the two temperature signals, by the chip speed ( $v_{ch}$ ) calculated by equation 2 from a measured exemplary chip thickness.

Figure 6 shows the spot positions on the chip surface. The spots are focused close to the vicinity of the chip. At this position the chip is in good approximation parallel to the tool surface. The angle of incidence can be chosen small enough to avoid any disturbances by chip vibrations.

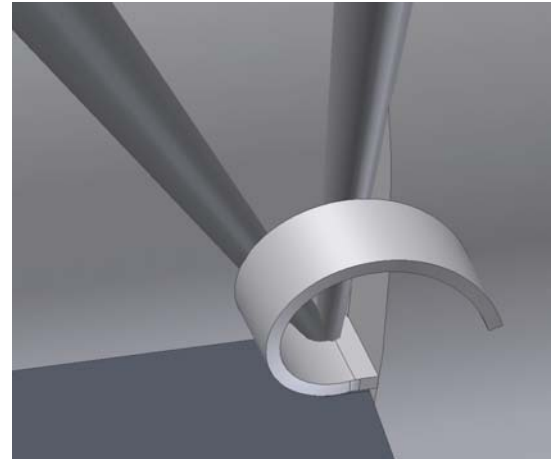


Figure 6: Spot positioning on the chips upper surface.

### 3.3 Fibre Optics Pyrometer

In the present work fibre optics pyrometer of type Kleiber 274-LWL were used. This type of pyrometer consists of 3 parts: an optical head, a glass fibre and a signal processing unit. The radiation, coming from the optical head, is transported through the glass fibre to the converter. The pyrometer lens is in a safe distance from the machining process. This arrangement allows measurements under difficult access conditions [18].

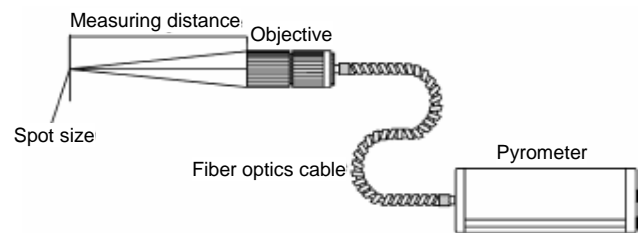


Figure 7: Fibre optics Pyrometer.

The main characteristics of the applied optical system are:

- Response time: 10  $\mu$ s.
- Measuring distance: 50 mm.
- Minimum spot sizes: 0.5 mm.
- Temperature range: 200 ... 1000°C.
- Spectral range: 1.58 ... 2.2  $\mu$ m.

Because of the small spot size, sufficient small distances ( $ds$  in the order of 1 mm) can be achieved. The broad temperature range and the high dynamic given by the short response time guarantee a measurement signal as long as chip is in focus.

### 3.4 Pyrometer cone calibration

The optics of a pyrometer transmits the image of a section of the target area of the measured surface to the detector. This section is called the spot size [18], and it depends on the distance between the surface and the optic, creating a cone. The geometrical information about the spot cone is given by the pyrometer manufacturer in a table or in a diagram format.

To be able to use fibre optics pyrometer in machining environment the optics must be protected against hot chips, dust and oil. Therefore quartz plain lenses were positioned in front of the optics. However these new lenses changed the cone size and length, demanding a calibration. The calibration was done moving a heat source with a constant speed ( $v_f$ ), parallel to the optic and measuring the temperature signals. Combining the ( $v_f$ ) and the temperature signals it was possible to define the spot diameter at this position (Figure 8 and 9).

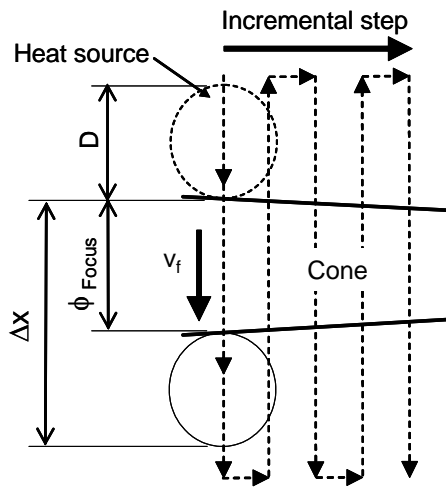


Figure 8: Optical cone calibration.

Repeating this procedure at different distances from the optics, it was possible to achieve the new spot cone.

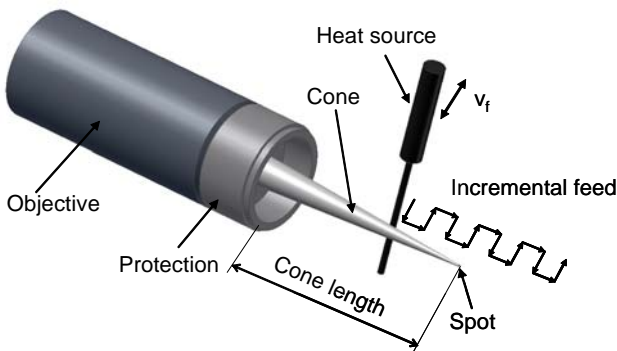


Figure 9: Construction of the new spot cone.

### 3.5 Measurement errors

The Figure 10 shows how the measurement distance ( $ds$ ) is affected by a chip thickness variation during the cutting process. This effect can be calculated with a geometrical relation of the chip thickness, the pyrometer's construction and pyrometer's positioning Equation 5.

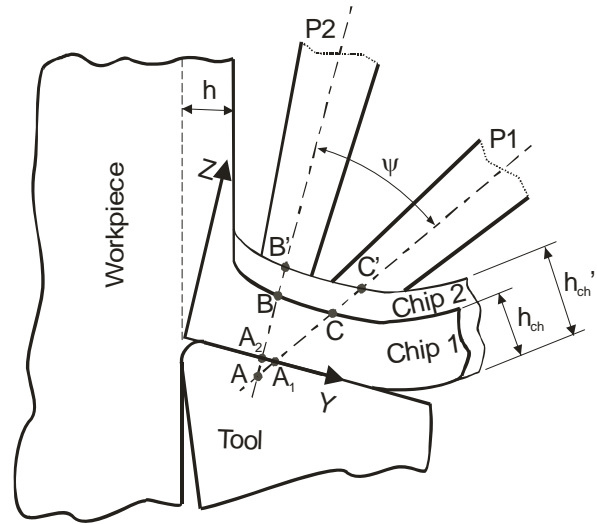


Figure 10: Influence of chip thickness on the measurement distance.

Where:

$$ds = \overline{BC} = \text{Measurement distance.}$$

$$ds'(h_{ch}') = \overline{B'C'} = \frac{(h_{ch}' + \overline{AA_2})}{(h_{ch} + \overline{AA_2})} \cdot ds \quad (5)$$

The chip flow direction ( $\eta_s$ ) has also an influence on the chip velocity monitoring Figure 11. If the chip flows straight, the parallel temperature profiles of the chip can be measured by both pyrometers with a time delay proportional to the measurement distance and the chip velocity. If the chip flows with a curling shape these profiles are deformed and the measurement distance/time relation can not be applied.

The equations 6 and 7 are used to estimate the measurement error if the chip side-flow angle ( $\eta_s$ ) has a big variation during the trails.

$$ds'(\eta_s, \eta_s') = \overline{BE} = \frac{\cos(\eta_s') \cdot ds}{\cos(\eta_s)}, \text{ if } \eta_s' > \eta_s \quad (6)$$

$$ds'(\eta_s, \eta_s') = \overline{BE} = \frac{\cos(\eta_s) \cdot ds}{\cos(\eta_s')}, \text{ if } \eta_s' < \eta_s \quad (7)$$

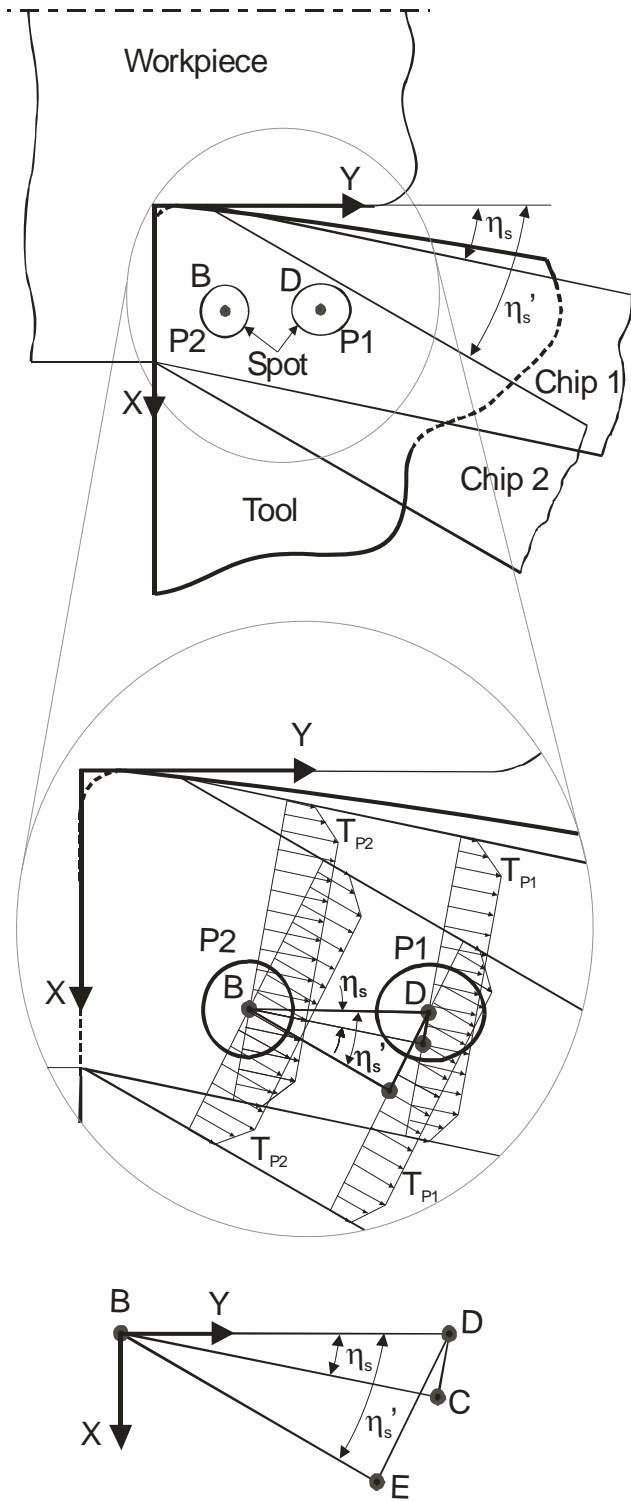


Figure 11: Chip flow direction influence on the measurement distance.

Where:

$\eta_s$  = Chip side-flow angle for chip 1.

$\eta_s'$  = Chip side-flow angle for chip 2.

$T_{P1}$  = Temperature profile in point D.

$T_{P2}$  = Temperature profile in point B.

$ds = \overline{BC}$  = Measurement distance.

#### 4 EXPERIMENT AND ANALYSES

In all tests 500 mm long bright bars with 31 mm diameter were used. The machining parameters of the single point turning tests were:

- Depth of cut ( $a_p$ ) = 2 mm.
- Feed rate ( $f$ ) = 0.2 mm/rev.
- Cutting speed ( $v_c$ ) = 200, 250 and 315 m/min.

Three different low carbon free cutting steels were considered in the on-line chip speed evaluation:

	C	S	Mn	Si	P	Bi	Sn
Steel 1	0.09	0.38	1.47	0.16	0.011	-	-
Steel 2	0.09	0.31	1.03	0.003	0.062	0.078	-
Steel 3	0.09	0.30	1.13	0.006	0.058	-	0.054

Table 1: Material compositions [%].

Steel 1 is an inclusion engineered steel. The silicate inclusions in this steel grade are expected to be glassy leading to a lubricating effect in the chip tool interface [19].

##### 4.1 Calibration of $ds$

All materials were turned 15 times with 200, 250 and 315 m/min cutting speed, 2 mm depth of cut and 0.2 mm cutting feed.

Parallel to the on-line measurement thirty chips were collected manually to measure their thicknesses with a caliper (Table 2).

Material	$v_c$ [m/min]	$\overline{h_{ch}}$ [mm]	$\sigma_{h_{ch}95}$ [mm]
Steel 1	200	0.416	0.005
Steel 2		0.425	0.006
Steel 3		0.441	0.008
Steel 1	250	0.413	0.004
Steel 2		0.424	0.007
Steel 3		0.428	0.008
Steel 1	315	0.397	0.005
Steel 2		0.401	0.004
Steel 3		0.407	0.008

$\sigma_{h_{ch}95}$  = Standard deviation for 95% confidence level.

Table 2: Chip thickness measurement.

The statistical method applied is resumed by Equation 8 to 11 [20].

$$\overline{h_{ch}} = \frac{\sum h_{ch_i}}{n} \quad (8)$$

$$s_{h_{ch}} = \pm \sqrt{\frac{\sum (h_{ch_i} - \overline{h_{ch}})^2}{n-1}} \quad (9)$$

$$\sigma_{h_{ch,95}} = \pm(t_{95} \cdot s_{h_{ch}}) \quad (10)$$

$$\sigma_{h_{ch,95}} = \pm \frac{\sigma_{h_{ch,95}}}{\sqrt{n}} \quad (11)$$

Where [20]:

$$n = 30.$$

$$t_{95} = 2.05.$$

The temperature signals were cross correlated obtaining the time delay ( $dt$ ). With equations 2 and 4 and statistical methods, the measurement distance ( $ds$ ) was calculated for a reference material (steel 1) and a reference cutting speed (200 m/min).

$v_c$ [m/min]	$\overline{ds}$ [mm]	$u_{ds95}^-$ [mm]
200	1.57	0.07

Table 3: Calibration of measurement distance  $ds$ .

Where  $u_{ds95}^-$  is the uncertainty of measurement and can be calculated with the Equation 12 [20].

$$u_{ds95}^- = \pm \sqrt{\left( \frac{\delta \overline{ds}}{\delta dt} \cdot \sigma_{dt95}^- \right)^2 + \left( \frac{\delta \overline{ds}}{\delta v_{ch}} \cdot \sigma_{v_{ch}95}^- \right)^2} \quad (12)$$

#### 4.2 On-line measurements

In order to avoid influence of wear on the chip speed, all turning operations were done with a new cutting edge from a TiN coated hard metal insert with geometry (CNMG120408). No coolant was used.

The external single point turning operation was done on a workpiece with initially 31 mm diameter. Each cutting process was 15 mm length, enough for a stable chip formation. Five workpieces were used for each combination of parameters, permitting a statistical analysis of the temperature signals.

As an example, figure 12 shows the filtered temperature signals from both pyrometers when turning steel 1. It can be seen that the temperature signals are delayed between themselves.

Applying the cross correlation the time delay is obtained (Figure 13).

The chip speeds values, obtained by the on-line and off-line measurements, are compared in the Figure 14. The diagonal line represents an ideal consistence between the two data sets.

The on-line method tends to underestimate the chip speed. This can be understood taking into account the chip curvature. The assumption of a planar distance ( $ds$ ) becomes incorrect if the radius of chip curvature gets small. Due to thermal gradients the curvature radius is expected to decrease with increasing cutting speeds. This leads to an underestimation of ( $ds$ ) at higher cutting speeds resulting in an underestimation of the chip velocity. In spite of those variations, the on-line measurement errors are not more than 22 % (Table 4).

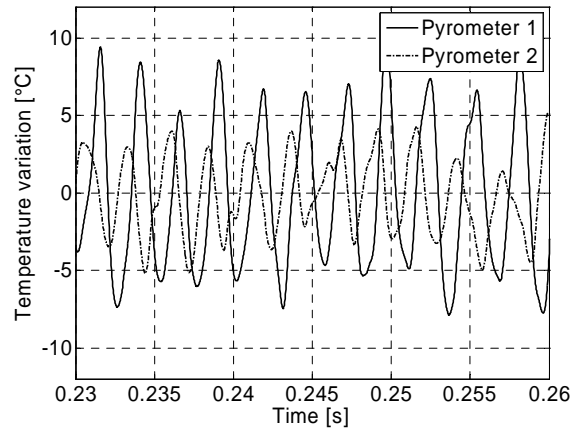


Figure 12: Chip temperature signals during turning process.

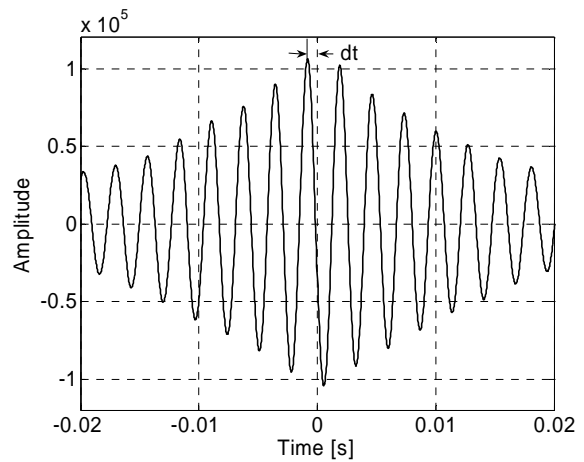


Figure 13: Cross correlation of the temperature signals.

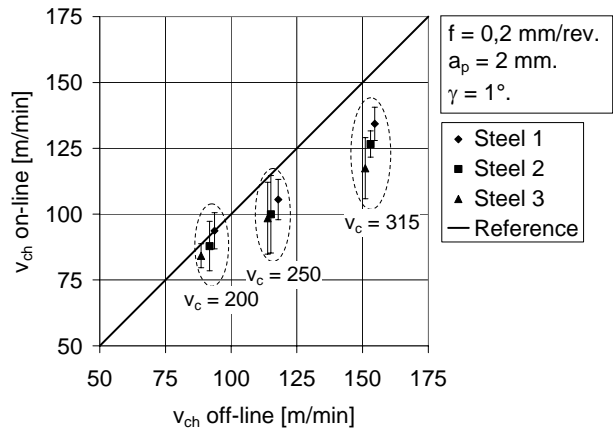


Figure 14: On-line and off-line chip speed measurements.

$v_c$ [m/min]	Steel 1	Steel 2	Steel 3
200	0	4	5
250	12	13	14
315	15	17	22

Table 4: Measurement error [%].

The uncertainty of the on-line measurement is dependent on the cutting speed and on the workpiece material. The chip speed of steel 1 is less affected by the cutting speed. The shear angle values, obtained by the on-line chip speed measurements are presented in Figure 15.

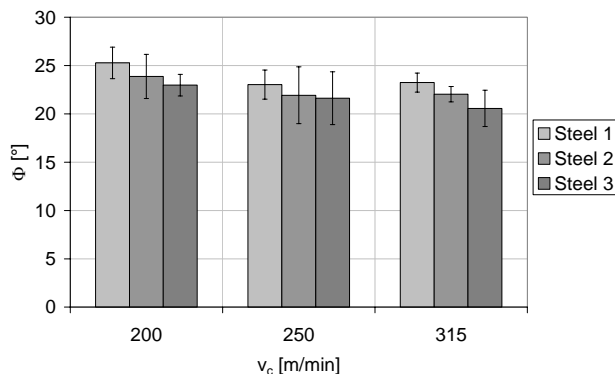


Figure 15: On-line measurements of shear angle.

In the on-line experiments the steel 1 has the highest chip velocity (Figure 14) and the largest shear angle (Figure 15) which is explained by the presence of lubrication inclusions in this steel. This result was off-line verified by the chip thickness (Table 2).

As an example Figure 16 shows a comparison between the on and off-line shear angle measurements when turning the steel 2.

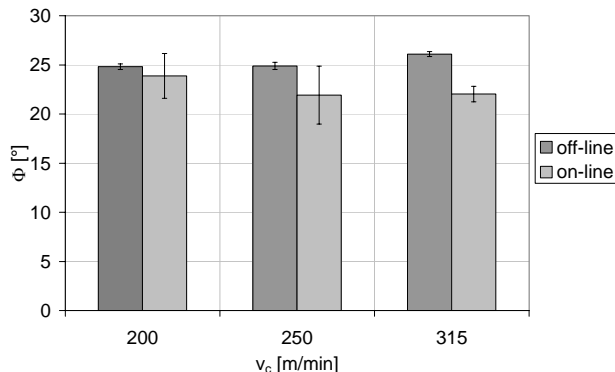


Figure 16: Shear angle steel 2.

## 5 CONCLUSIONS

Applying modern fibre optics pyrometers a new method for on-line characterization of the turning process has been developed. The method can be used to measure the chip velocity at the vicinity of shear plane.

Chip thickness and shear angle can be deduced from chip velocity by simple geometrical relationships.

Further developments concern an improvement of stiffness of the construction, an improvement of positioning of the pyrometer spots on the chip surface. Higher data accuracy will also be achieved due a better understanding of the temperature signals.

## 6 ACKNOWLEDGMENTS

This research was supported by von Moos Stahl AG, Blaser Swisslube, Iscar Hartmetall AG and the commission for technology and innovation (CTI). The Authors would like to thank them for there cooperation.

## 7 REFERENCES

- [1] ISO 3685, 1993, Tool-life testing with single-point turning tools, 2<sup>nd</sup> Edition.
- [2] Kuster, F., Margot, R., 2002, Online-Spanlängenerkennung beim Drehen, SMM Schweizer Maschinenmarkt, 45:93-95.
- [3] British Steel, 1999, Development of a new machinability test methodology/machining model for improved free cutting steels, ECSC research contract 7210.MA/821, EUR 18617.
- [4] Childs, T.H.C., et al, 2000, Metal Machining: Theory and Applications, Arnold, London.
- [5] Jaspers, S.P.F.C., Dautzenberg, J.H., 2002, Material behaviour in metal cutting: strains, strain rates and temperatures in chip formation, Journal of Materials Processing Technology, 121:123-135.
- [6] Leopold, J., 2000, The Application of Visioplasticity in Predictive Modelling the Chip Flow, Tool Loading and Surface Integrity in Turning Operations, 3<sup>rd</sup> CIRP International Workshop on "Modelling of Machining Operations", 1-13.
- [7] Stemmer, C.E., 1995, Ferramentas de Corte I, 4<sup>th</sup> Edição, Editora da UFSC, Florianópolis.
- [8] König, W., Klocke, F., 1997, Fertigungsverfahren: Drehen, Fräsen, Böhren, 4<sup>th</sup> Edition, VDI-Verlag, Düsseldorf.
- [9] Altintas, Y., 2000, Manufacturing Automation: Metal Cutting Mechanics, Machine Tools Vibrations, and CNC Design, Cambridge University Press, Cambridge.
- [10] Boothroyd, G., Knight, W.A., 1989, Fundamentals of Machining and Machine Tools, 2<sup>nd</sup> Edition, Marcel Dekker, New York.
- [11] Trent, E.M., Wright, P.K., 2000, Metal Cutting, 4<sup>th</sup> Edition, Butterworth-Heinemann.
- [12] Jawahir, I.S., van Luttervelt, C.A., 1993, Recent Developments in Chip Control Reserch and Applications, Annals of the CIRP, 42/2:659-693.
- [13] Qi, H.S., Mills, B., 2000, Formation of a transfer layer at the tool-chip interface during machining, Wear, 245:136-147.
- [14] Kluff, W., König, W., et al, 1979, Present Knowledge of Chip Control, Annals of the CIRP, 28/2:441-455.
- [15] Cahuc, O., et al, 2001, Experimental and Analytical Balance Sheet in Turning Applications, International Journal Advanced Manufacturing Technology, 18:648-656.
- [16] [http://www.informatik.fh-wiesbaden.de/~linn/vpdv9900/ortgKorr/kk\\_why.html](http://www.informatik.fh-wiesbaden.de/~linn/vpdv9900/ortgKorr/kk_why.html).
- [17] <http://mathworld.wolfram.com/Cross-Correlation.html>.
- [18] Pauly, H., Engel, F., 1999, Das Pyrometer-Kompedium, Quickdruck, Frankfurt am Main.
- [19] Zhang, X., et al, 2004, Application of Thermodynamic Model for Inclusion Control in Steelmaking to Improve the Machinability of Low Carbon Free Cutting Steels, Steel Research International 75, 5:314-321.
- [20] Bantel, M., 2000, Grundlagen der Messtechnik, Carl Hansen Verlag.